Supporting Information

Structure-Activity Relationships of Copper- and Potassium-Modified Iron Oxide Catalysts during Reverse Water-Gas Shift Reaction

Mengwei Gu[a,#], Sheng Dai[b,#], Runfa Qiu[a], Michael E. Ford[c], Chenxi Cao[d], Israel E. Wachs[c] and Minghui Zhu[a,*]

[a] State Key Laboratory of Chemical Engineering, School of Chemical Engineering, East China University of Science and Technology, Shanghai 200237, China

[b] Key Laboratory for Advanced Materials and Feringa Nobel Prize Scientist Joint Research Center, School of Chemistry and Molecular Engineering, East China University of Science and Technology, Shanghai 200237, China

[c] *Operando* Molecular Spectroscopy & Catalysis Laboratory, Department of Chemical and Biomolecular Engineering, Lehigh University, Bethlehem, Pennsylvania 18015, United States

[d] Key Laboratory of Smart Manufacturing in Energy Chemical Process, Ministry of Education, East China University of Science and Technology, Shanghai 200237, China

Corresponding E-mail: minghuizhu@ecust.edu.cn

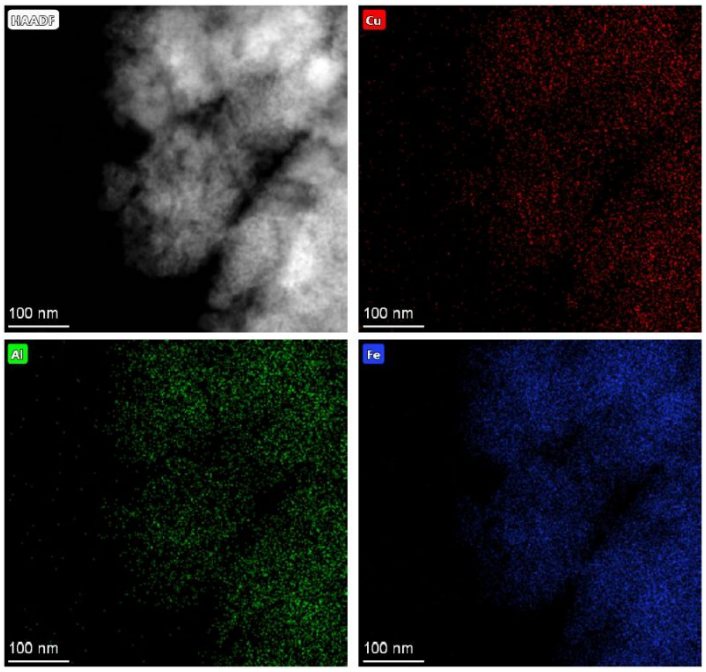

Figure S1. HAADF-STEM image of fresh CuAlFe and the corresponding elemental maps of Cu, Al, and Fe.

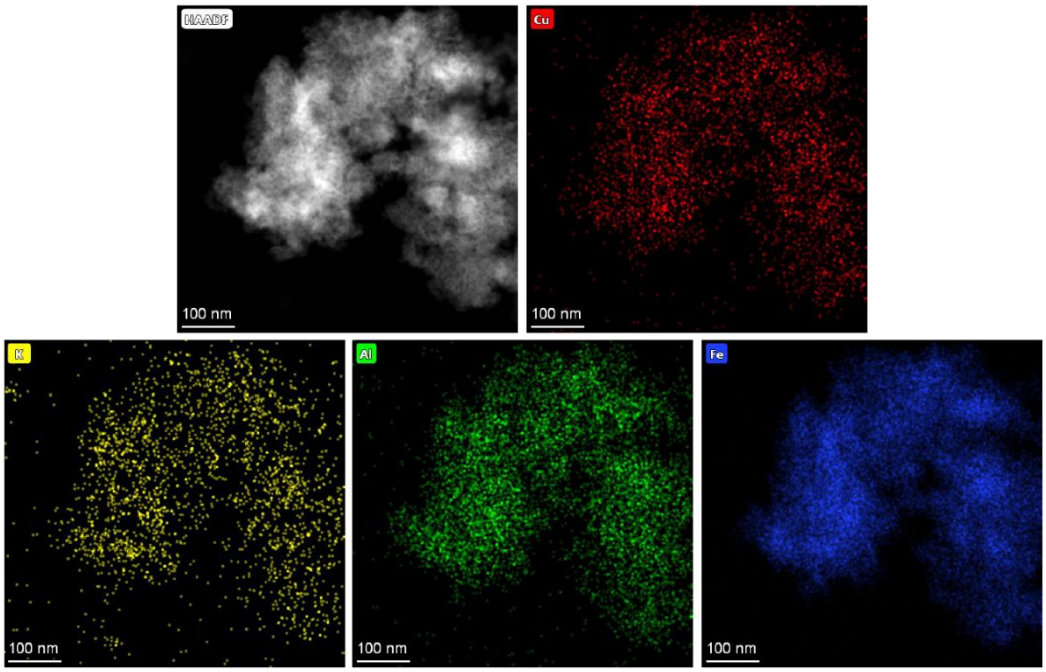

Figure S2. HAADF-STEM image of fresh KCuAlFe and the corresponding elemental maps of Cu, K, Al, and Fe.

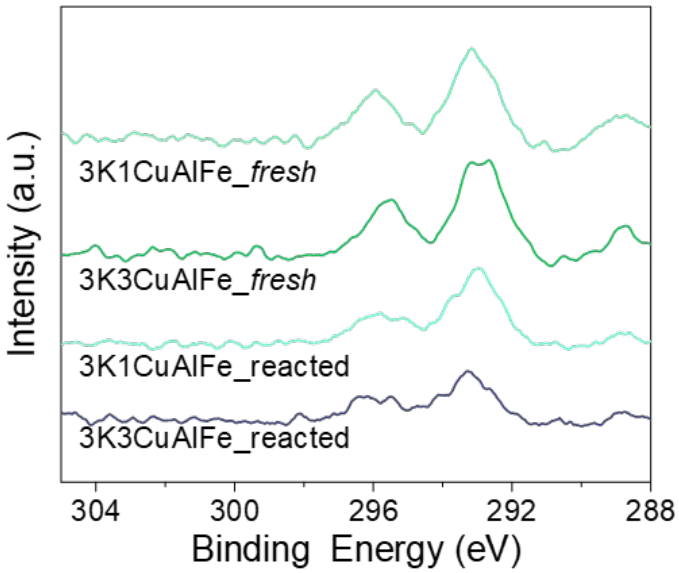

Figure S3. Quasi *in situ* XPS spectrum of the KCuAlFe catalysts showing the K 2p regions.

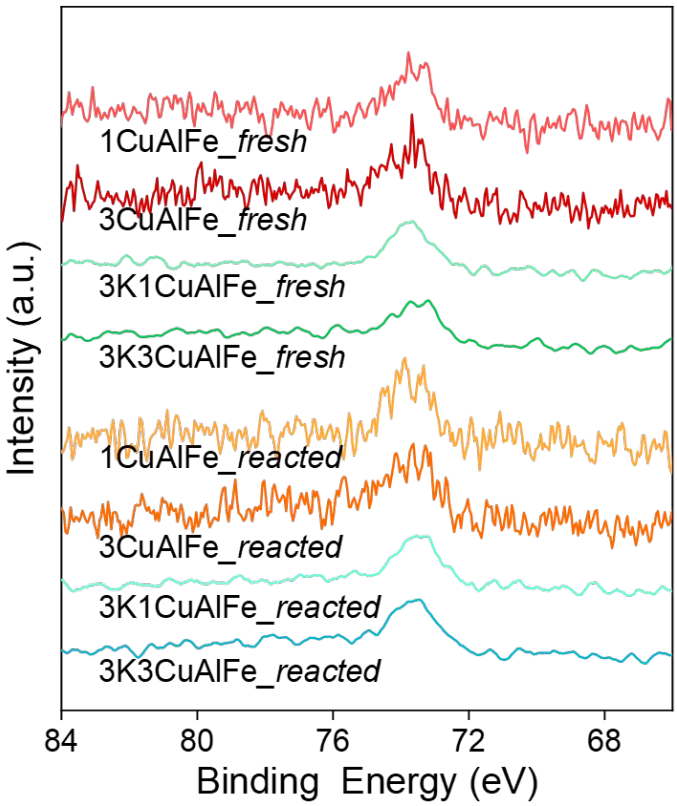

Figure S4. Quasi *in situ* XPS spectra of the fresh iron-based catalysts showing the Al 2p regions.

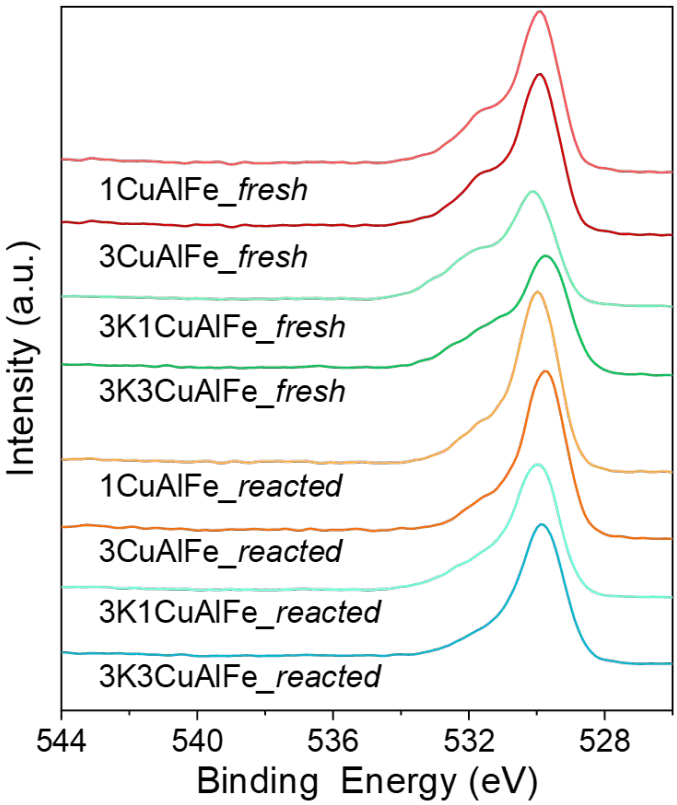

Figure S5. Quasi *in situ* XPS spectra of the iron-based catalysts showing the O 1s regions.

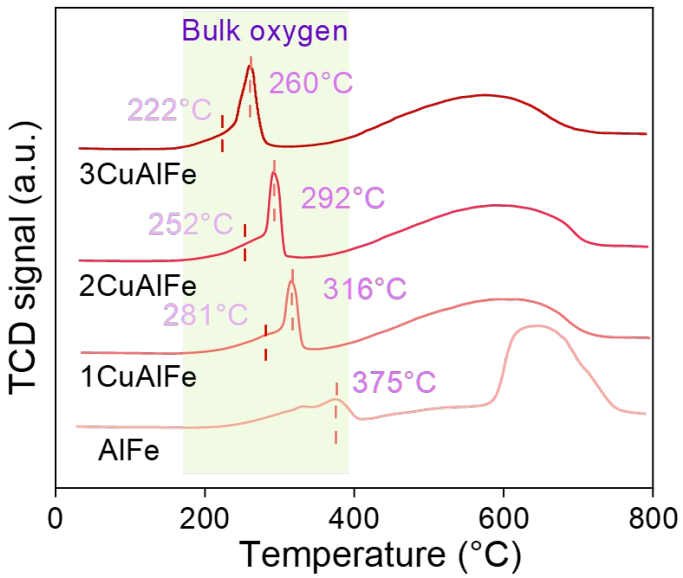

Figure S6. H_2-TPR profiles of the fresh *n*CuAlFe catalysts.

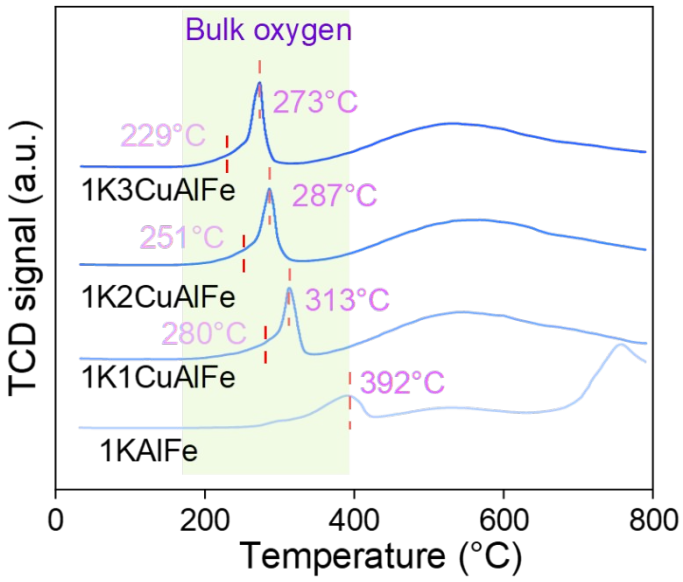

Figure S7. H_2-TPR profiles of the fresh 1K*n*CuAlFe catalysts.

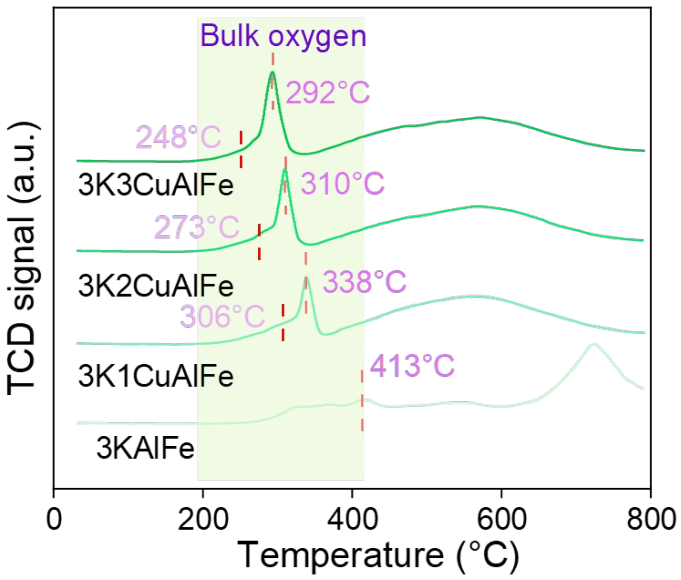

Figure S8. H_2-TPR profiles of the fresh 3K*n*CuAlFe catalysts.

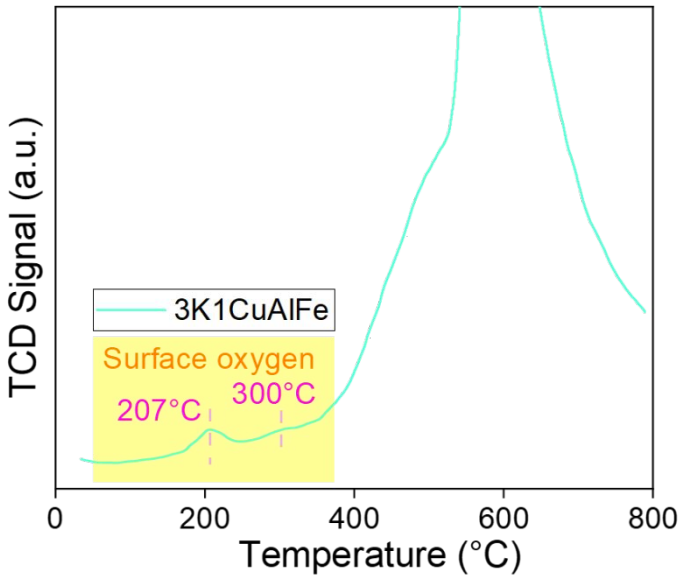

Figure S9. H_2-TPR profiles of the reaction-treated 3K1CuAlFe catalysts.

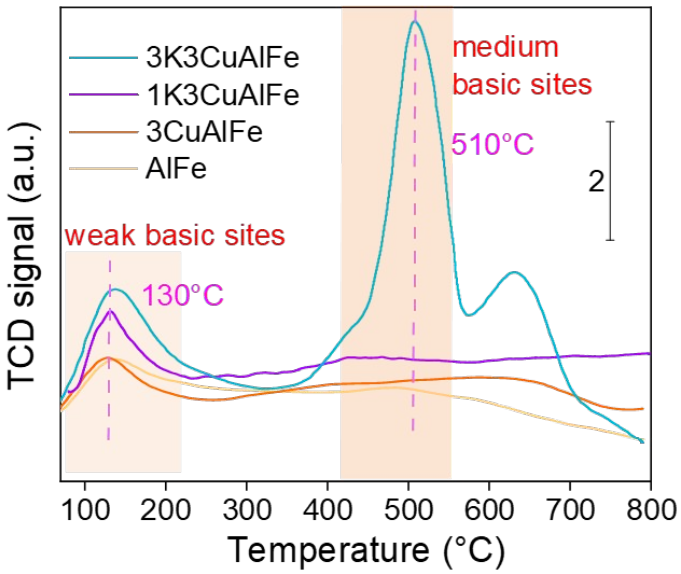

Figure S10. CO_2-TPD profiles of the reaction-treated AlFe, 3CuAlFe,1K3CuAlFe and 3K3CuAlFe.

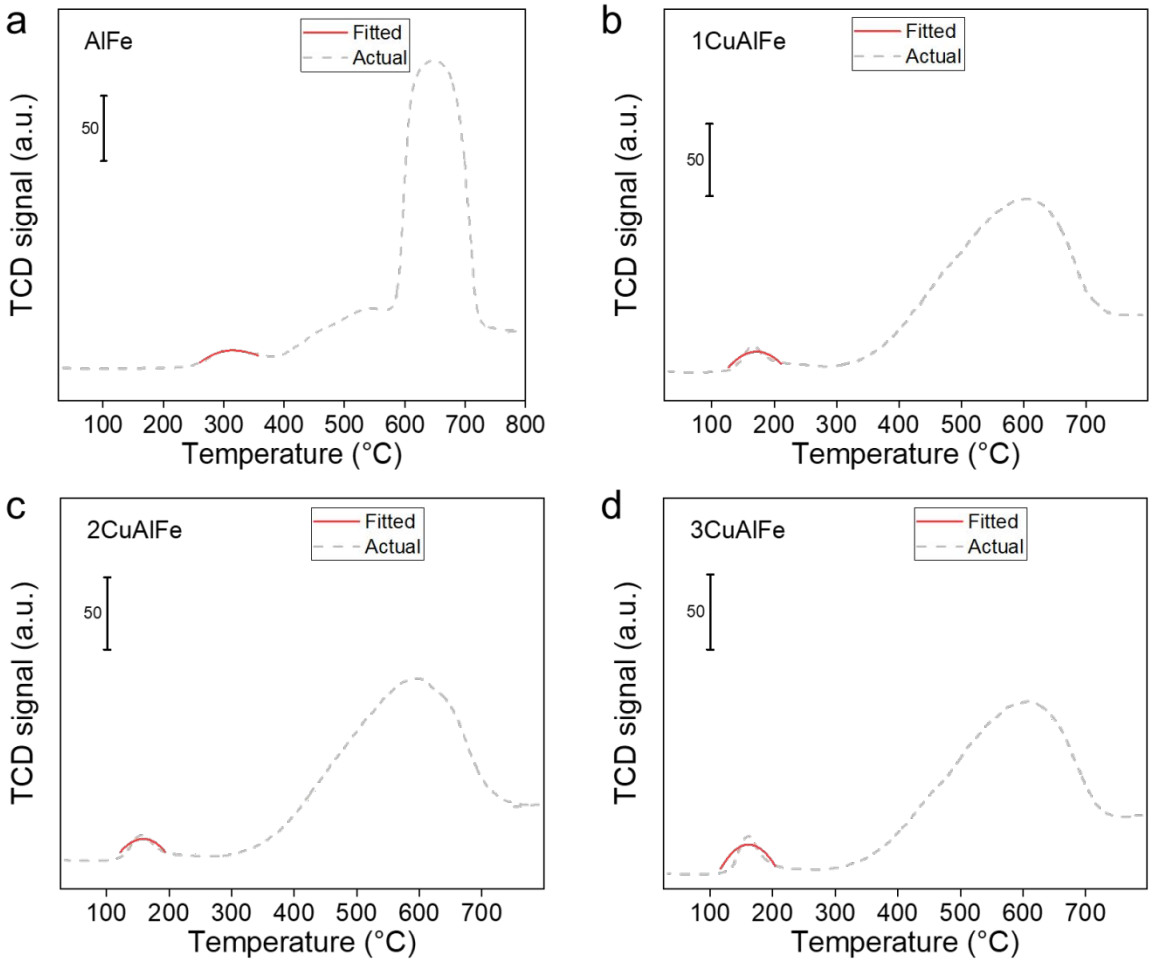

Figure S11. Actual and fitted reduction peaks for reaction-treated (a) AlFe, (b) 1CuAlFe, (c) 2CuAlFe and (d) 3CuAlFe.

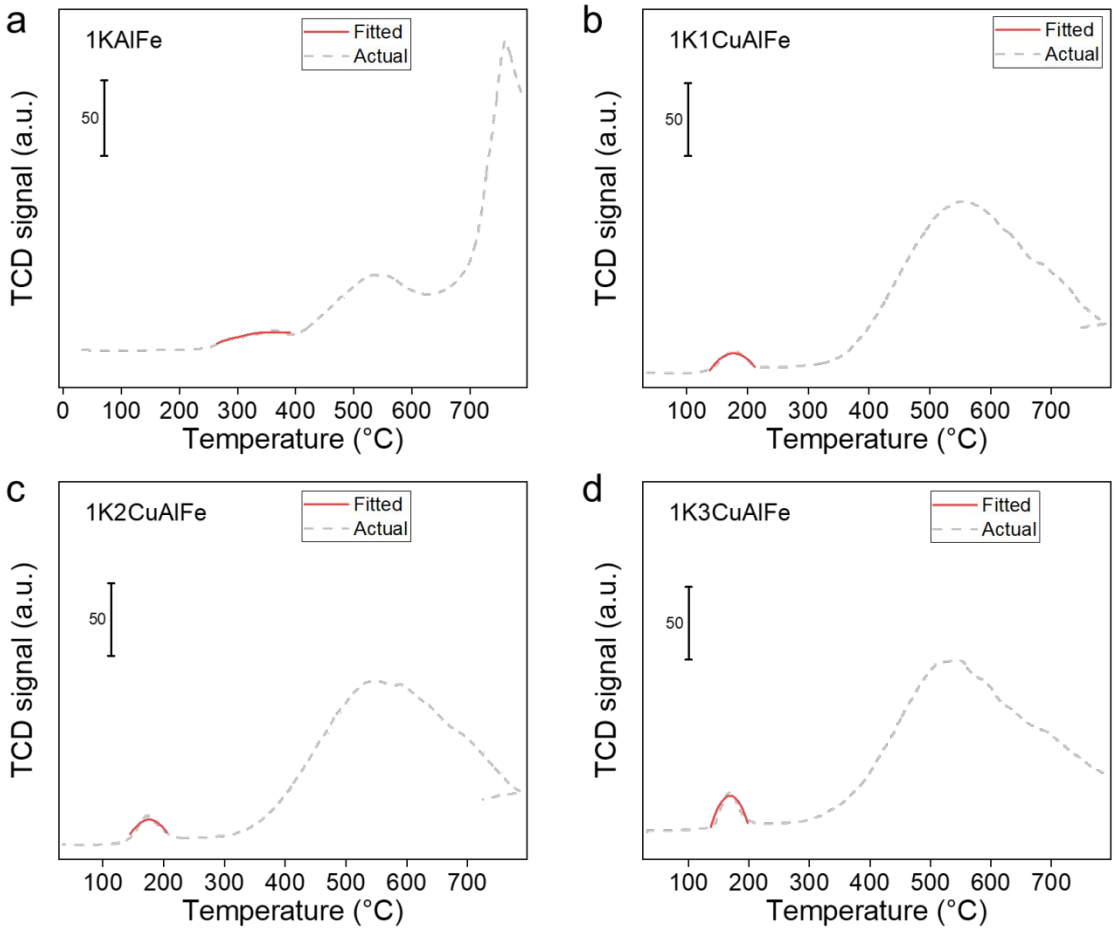

Figure S12. Actual and fitted reduction peaks for reaction-treated (a) 1KAlFe, (b) 1K1CuAlFe, (c) 1K2CuAlFe and (d) 1K3CuAlFe.

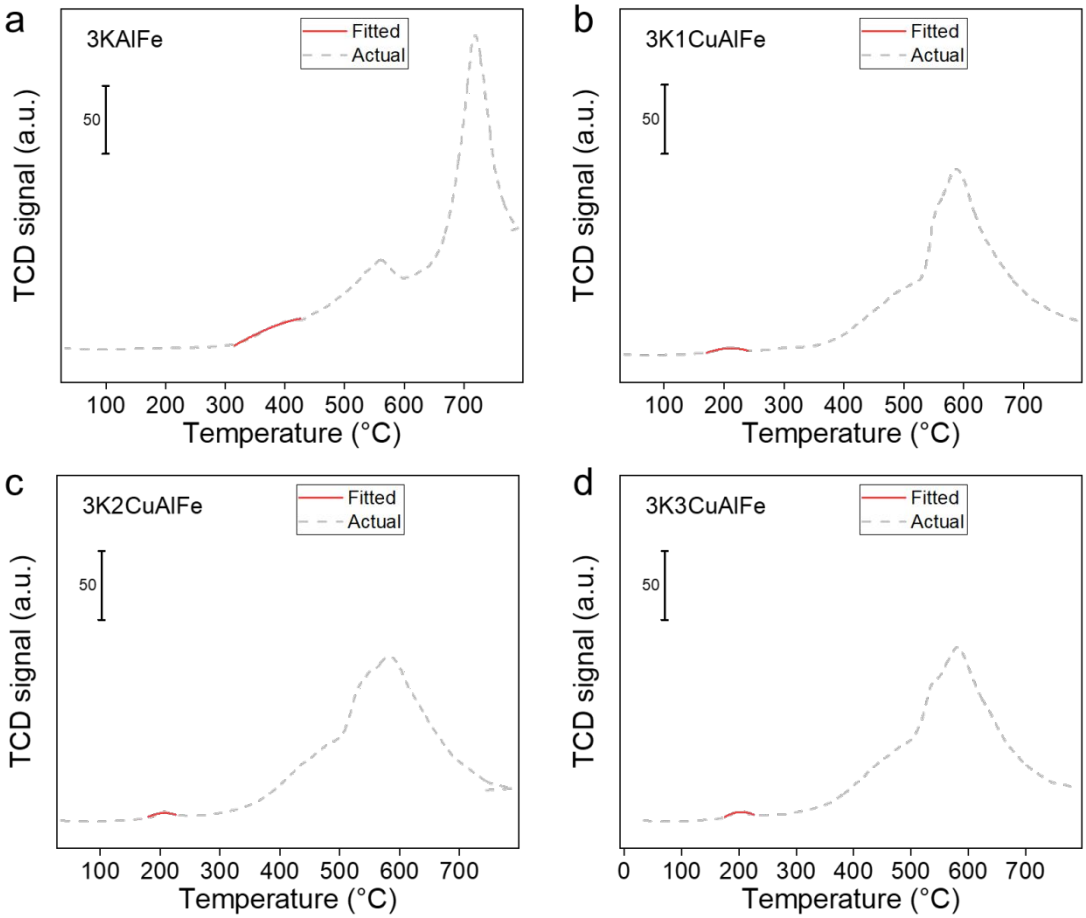

Figure S13. Actual and fitted reduction peaks for reaction-treated (a) 3KAlFe, (b) 3K1CuAlFe, (c) 3K2CuAlFe and (d) 3K3CuAlFe.

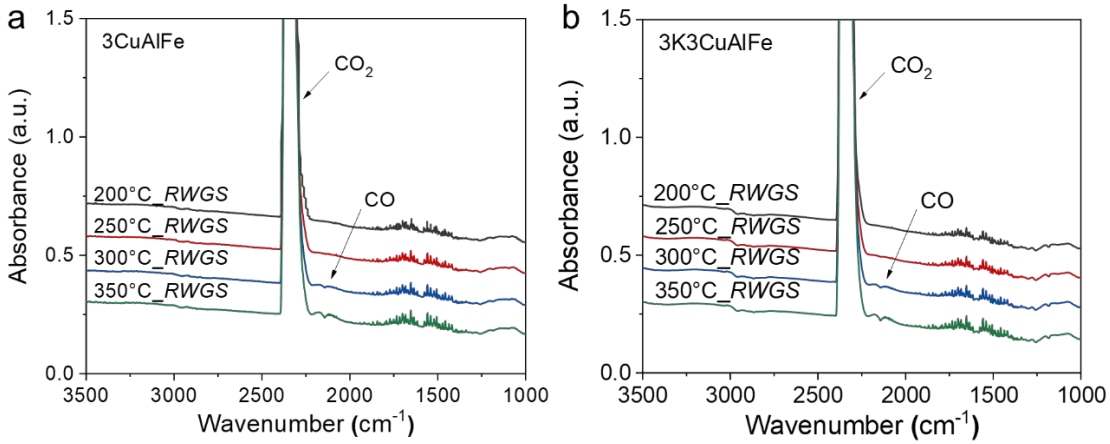

Figure S14. In situ DRIFTS spectra of (a) 3CuAlFe and (b) 3K3CuAlFe during the RWGS reaction at various temperatures.

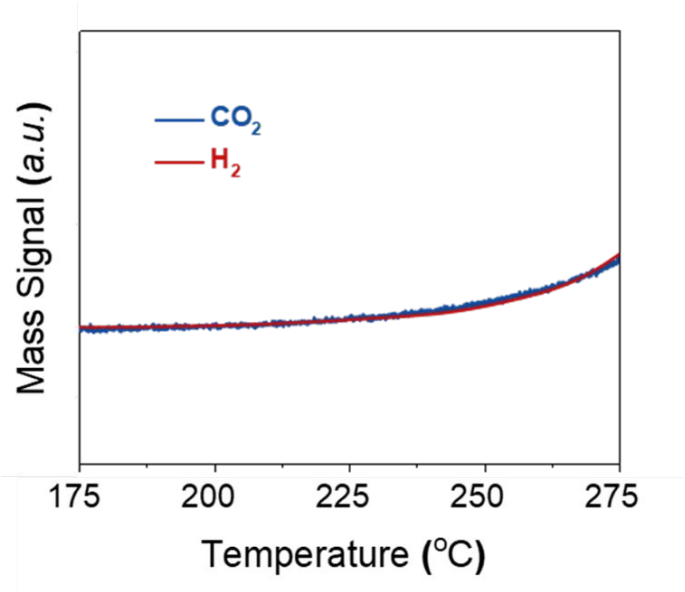

Figure S15. Evolution of CO_2 (m/z=44) and H_2 (m/z=2) signals during the HCOOH-TPSR over the activated 3CuAlFe catalyst.

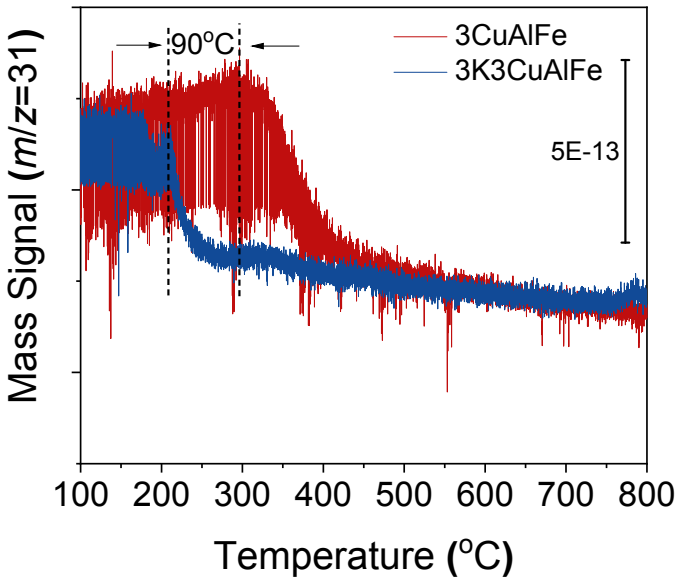

Figure S16. Consumption of HCOOH (m/z=31) during the HCOOH-TPSR over activated 3CuAlFe and 3K3CuAlFe catalysts.

Table S1. Nominal compositions of the fresh catalysts

Catalyst	Contents (wt.%)			
	K_2O	CuO	Al_2O_3	Fe_2O_3
AlFe	0	0	8	92
1CuAlFe	0	1	8	91
2CuAlFe	0	2	8	90
3CuAlFe	0	3	8	89
1KAlFe	1	0	8	91
1K1CuAlFe	1	1	7.8	90.2
1K2CuAlFe	1	2	7.8	89.2
1K3CuAlFe	1	3	7.8	88.2
3KAlFe	3	0	8	89
3K1CuAlFe	3	1	7.8	88.2
3K2CuAlFe	3	2	7.8	87.2
3K3CuAlFe	3	3	7.8	86.2

Table S2. The BET surface area, Barrett Joiner Halenda (BJH) pore volume, and pore size of the fresh CuAlFe and KCuAlFe catalysts.

Catalyst	BET Surface Area (m^2/g)	Pore Volume (cm^3/g)	Pore Size (nm)
AlFe	133.2	0.21	4.80
1CuAlFe	152.9	0.20	3.77
3CuAlFe	173.7	0.34	4.35
3KAlFe	108.9	0.18	4.91
3K1CuAlFe	140.0	0.18	3.75
3K3CuAlFe	154.1	0.32	4.66

Table S3. The BET surface area, Barrett Joiner Halenda (BJH) pore volume, and pore size of the reaction-treated CuAlFe and KCuAlFe catalysts.

Catalyst	BET Surface Area (m^2/g)	Pore Volume (cm^3/g)	Pore Size (nm)
AlFe	51.8	0.15	8.15
1CuAlFe	47.6	0.13	7.49
3CuAlFe	51.0	0.15	8.41
3KAlFe	58.3	0.14	6.96
3K1CuAlFe	52.0	0.13	8.12
3K3CuAlFe	49.5	0.15	9.93

Table S4. The crystallite size and lattice parameters of the catalysts according to *in situ* XRD catalysis.

Catalyst	Crystallite size(nm)	Lattice parameters (Å)		
		a	b	c
AlFe_fresh	8.8	4.9980	4.9980	13.8123
3KAlFe_fresh	15.0	5.0022	5.0022	13.8129
3CuAlFe_fresh	12.5	4.9956	4.9956	13.7774
3K3CuAlFe_fresh	10.8	5.0023	5.0023	13.7851
3CuAlFe_reacted	12.3	8.4000	8.4000	8.4000
3K3CuAlFe_reacted	12.9	8.3819	8.3819	8.3819

Table S5. Surface atomic ratio of each element in the fresh catalysts according to Quasi *in situ* XPS catalysis.

Catalyst	Al	Cu	Fe	K	O
1CuAlFe	5.35	2.58	30.00	/	62.05
3CuAlFe	6.46	3.07	31.33	/	59.12
3K1CuAlFe	11.41	1.77	25.20	2.55	59.07
3K3CuAlFe	11.89	2.51	25.55	2.69	57.35

Table S6. Surface atomic ratio of each element in the reaction-treated catalysts according to Quasi *in situ* XPS catalysis.

Catalyst	Al	Cu	Fe	K	O
1CuAlFe	5.72	2.34	37.99	/	53.94
3CuAlFe	8.04	2.37	36.08	/	53.49
3K1CuAlFe	12.48	1.87	33.66	1.31	50.67
3K3CuAlFe	15.09	2.27	31.46	1.82	49.36

Table S7. Number of surface redox oxygens (Ns_r) and $[k_r]_{350°C}$ after reaction treatment, as well as the steady-state RWGS activities of iron-based catalysts.

Catalyst	Ns_r ($\times 10^{-4}$ mol/g)	$[k_r]_{350°C}$ (s^{-1})	Activity (μmol CO_2/s·g)
AlFe	5.1657	0.0174	3.99
1CuAlFe	6.9376	16.3948	13.19
2CuAlFe	7.2962	18.8679	14.83
3CuAlFe	9.3874	19.6605	17.72
1KAlFe	5.6900	0.0028	4.35
1K1CuAlFe	4.8722	10.3688	22.03
1K2CuAlFe	7.1888	12.4245	23.06
1K3CuAlFe	7.2863	14.5106	24.05
3KAlFe	2.7653	0.0012	1.44
3K1CuAlFe	1.1638	4.0361	13.63
3K2CuAlFe	1.1702	4.5632	12.25
3K3CuAlFe	1.0504	5.7299	13.78

Table S8. Number of weak basic sites (Ns_{wb}) and medium basic sites (Ns_{mb}) of iron-based catalysts after reaction treatment.

Catalyst	Ns_{wb} (mmol/g)	Ns_{mb} (mmol/g)
AlFe	1.70	--
1CuAlFe	0.95	--
2CuAlFe	1.18	--
3CuAlFe	1.38	--
1KAlFe	1.76	0.53
1K1CuAlFe	2.09	0.66
1K2CuAlFe	1.88	0.56
1K3CuAlFe	1.91	0.67
3KAlFe	3.92	2.51
3K1CuAlFe	3.29	5.75
3K2CuAlFe	3.29	7. 90
3K3CuAlFe	3.27	8.69